

Identification of Zn-vacancy–hydrogen complexes in ZnO single crystals: A challenge to positron annihilation spectroscopy

G. Brauer, W. Anwand, D. Grambole, J. Grenzer, and W. Skorupa

Institut für Ionenstrahlphysik und Materialforschung, Forschungszentrum Dresden-Rossendorf, Postfach 510119, D-01314 Dresden, Germany

J. Čížek, J. Kuriplach, and I. Procházka

Department of Low Temperature Physics, Faculty of Mathematics and Physics, Charles University, V Holešovičkách 2, CZ-180 00 Prague, Czech Republic

C. C. Ling and C. K. So

Department of Physics, The University of Hong Kong, Pokfulam Road, Hong Kong, People's Republic of China

D. Schulz and D. Klimm

Institut für Kristallzüchtung, Max-Born-Str. 2, D-12489 Berlin, Germany

(Received 30 August 2008; revised manuscript received 11 February 2009; published 25 March 2009)

A systematic study of various, nominally undoped ZnO single crystals, either hydrothermally grown (HTG) or melt grown (MG), has been performed. The crystal quality has been assessed by x-ray diffraction, and a comprehensive estimation of the detailed impurity and hydrogen contents by inductively coupled plasma mass spectrometry and nuclear reaction analysis, respectively, has been made also. High precision positron lifetime experiments show that a single positron lifetime is observed in all crystals investigated, which clusters at 180–182 ps and 165–167 ps for HTG and MG crystals, respectively. Furthermore, hydrogen is detected in all crystals in a bound state with a high concentration (at least 0.3 at. %), whereas the concentrations of other impurities are very small. From *ab initio* calculations it is suggested that the existence of Zn-vacancy–hydrogen complexes is the most natural explanation for the given experimental facts at present. Furthermore, the distribution of H at a metal/ZnO interface of a MG crystal, and the H content of a HTG crystal upon annealing and time afterward has been monitored, as this is most probably related to the properties of electrical contacts made at ZnO and the instability in *p*-type conductivity observed at ZnO nanorods in literature. All experimental findings and presented theoretical considerations support the conclusion that various types of Zn-vacancy–hydrogen complexes exist in ZnO and need to be taken into account in future studies, especially for HTG materials.

DOI: [10.1103/PhysRevB.79.115212](https://doi.org/10.1103/PhysRevB.79.115212)

PACS number(s): 78.70.Bj

I. INTRODUCTION

Zinc oxide (ZnO), a wide band gap (~ 3.4 eV at 300 K) semiconductor material, is presently receiving worldwide attention because of fundamental advantages over GaN in the quest for blue/UV light emitters and detectors, as well as high-speed, high-power, high-temperature, and high-irradiation environment electronic devices.^{1–4} In spite of decades of study and recent progress in research on ZnO properties, there remain unresolved controversies which are mainly related to native defects formed during crystal growth. The crucial role of defects in semiconductor materials in controlling electrical and optical,⁵ as well as magnetic,^{6,7} properties has been well recognized. However, due to the variety of possible defects in compound semiconductors, and further complicated by the fact that native defects may exist on both sublattices and in different charge states, the interpretation of experimental results is not a trivial task. Thus, not only the combination of several methods is required to gain a better understanding of experimental findings but at the same time further development and inclusion of theoretical modeling into interpretation of any experimental data.

Identification of native defects and their role regarding a certain measurable property might be possible mainly at single crystals but is of special interest in the development of thin film and nanostructured applications based on ZnO—some examples are given in Refs. 8–10. A study of the Al₂O₃/ZnO interface⁸ has revealed that obviously Zn atoms are diffusing from ZnO into the covering oxide layer during annealing, and creation of deep level defects near the interface is observed. It shows that this interface is very fragile, and caution must be taken for making metal/oxide/ZnO-based transistors and light-emitting diodes. It is supposed that an open volume defect, connected with the Zn vacancy (V_{Zn}), is formed that needs to be identified. Very recently, a versatile method for the growth of *p*-type or *n*-type ZnO nanorods has been demonstrated,⁹ where the differences in conductivity type have been attributed to a dependency on native defect concentrations and hydrogen incorporation on the seed layer preparation method. The *p*-type conductivity has been attributed to an open volume defect, connected with V_{Zn} , and observed to be stable over a period of six weeks. Finally, light-emitting diodes with different device architectures based on the *p*-type ZnO nanorods could be demonstrated. However, an elucidation of the real structure of this

open volume defect, and the origin of the instability in *p*-type conductivity after some time, remain to be determined. Another very recent paper¹⁰ reports the fabrication of ZnO tetrapods of an exceptional optical quality, based on a photoluminescence (PL) lifetime in the range of tens of nanoseconds and the absence of defect emission. The observed PL lifetime for an optimal growth temperature of the ZnO tetrapods is found to be an order of magnitude higher than the best results achieved so far in ZnO epilayers and single crystals. From the comparison of given results with those obtained at ZnO single crystals of different origin, it has been concluded that intrinsic defects (most likely connected with V_{Zn}) rather than impurities play a major role in the obtained optical properties. However, the real structure of such intrinsic defects remains to be determined.

Positron annihilation spectroscopy (PAS),^{11,12} especially in the form of slow positron implantation spectroscopy (SPIS) using monoenergetic positrons,¹³ is now a well-established tool for the study of electronic and defect properties of bulk solids and thin films. A consistent theoretical modeling of bulk and defect positron properties of ZnO using the atomic superposition (ATSUP) method with and without lattice relaxation has been published recently.¹⁴ Later, positron lifetime data available in literature have been collected¹⁵ and been related to the values at Ref. 14. From this comparison,¹⁵ the idea of the existence of V_{Zn} -hydrogen complexes in ZnO sampled by positrons was born.

From Refs. 14 and 15 it becomes clear that the positron bulk lifetime τ_b varies within the broad range of 151–185 ps. Such a situation is quite unusual compared to other materials but points out that ZnO seems to be a rather special and difficult to understand material.

As early as in 1992, i.e., in connection with a systematic study of the possible origin of the green and yellow luminescence centers in 5N purity ZnO powders,¹⁶ the experimentally observed defect positron lifetime $\tau_d=(260 \pm 7)$ ps has been concluded to represent the neutral Zn+O divacancy. In our later work¹⁴ performed on a pair of ZnO single crystals obtained from Cermet Inc. (Atlanta/GA) (CM) we arrived by a combination of different methods at the same conclusion for the observed longer positron lifetime $\tau_2=(257 \pm 2)$ ps. A defect lifetime of about $\tau_d=(260 \pm 7)$ ps has also been observed to occur in a hydrothermally grown single crystal from CrysTec (Berlin) (CT) upon 3 MeV proton irradiation,¹⁷ which has been interpreted to be the Zn+O divacancy also.

Investigations¹⁸ of CT single crystals and those supplied from Eagle-Picher Inc. (Miami/FL) (EP) revealed only one positron lifetime component, declared to be the bulk lifetime, with values of $\tau_b=(173 \pm 2)$ ps and $\tau_b=(161 \pm 2)$ ps, respectively. However, the origin of the difference in these values was declared to be not fully understood at the moment, and that perhaps grown-in defects in the CT samples might be the most plausible cause. To further comment on this statement: if grown-in defects are the argument of observing such a difference in the “bulk lifetime” it is naturally to assume that the EP sample showing the much shorter “bulk lifetime” contains grown-in defects as well, i.e., the “true bulk lifetime” for a defect-free ZnO crystal has to be even shorter than (161 ± 2) ps.

Whereas from irradiation of CT samples with electrons of 1 MeV up to 5×10^{18} cm⁻² practically no change in the positron lifetime spectrum could be observed, an increase in the electron energy to 2 MeV resulted in an open volume defect-related positron lifetime of $\tau_d=(207 \pm 6)$ ps in CT and EP samples at various fluences up to 5×10^{18} cm⁻² (Ref. 18). This positron lifetime has been interpreted to be connected with V_{Zn} .

In a more recent review¹⁹ of experimental positron lifetime data obtained on a large variety of ZnO crystals, the interpretation of all given results is dominantly based on previous papers of the same authors^{20–22} where originally a value of $\tau_b=170$ ps has been derived. This has already been commented on in Ref. 14 in the sense that an adjustment of the calculation scheme²³ to give lifetimes for the bulk and Zn vacancy of 177 ps and 237 ps (Ref. 20), respectively, does not explain the previously observed defect characterized by a lifetime of $\tau_d=(207 \pm 6)$ ps (Ref. 18). Furthermore, the experimental positron lifetimes at V_{Zn} and even of an oxygen vacancy (V_{O}) in ZnO are given to be (230 ± 10) ps and (195 ± 5) ps, respectively. In the case of ZnO grown by a vapor phase technique (EP),²⁴ a single positron lifetime of 171 ps at room temperature is reported, which also has been observed at a material grown by the same technique but another company (ZN Technology, Brea/CA), or at ZnO grown by a pressurized melt method (Cermet Inc., Atlanta/GA)^{25,26} too. It might be reasonable to attribute the different findings¹⁴ on ZnO single crystals from the latter supplier to the much earlier date of purchase. However, the relevant *ab initio* calculations,^{14,27} which in particular show that V_{O} does not represent a trapping site for positrons, were not considered.

Furthermore, it is stated¹⁹ that the results and drawn conclusions obtained for ZnO single crystals from EP would coincide with those reported by two other groups having studied the same material.^{17,28} When looking up these two references it shows that there are reported values of $\tau_b=183–185$ ps and $\tau_b=155–158$ ps, respectively. Such differences are remarkable. The comment¹⁹ that slight differences in positron lifetime spectrometers—such as those between scintillators, geometry, and electronic settings—influence the absolute values of the positron lifetimes is certainly correct but should not be considered to be the only possible cause of the differences. Further sources of errors and thus differences in numerical results published by different laboratories have recently been discussed in Ref. 29.

In the review¹⁹ mentioned above, also hydrothermally grown ZnO single crystals from two different sources [Tokyo Denpa (Japan), and Scientific Production/Co. Goodwill (Russia)] have been investigated, and a single “average” lifetime of 180–185 ps is observed. Annihilations at possibly existing V_{O} (195 ps) have been considered as an explanation why these observed lifetimes are above the previously^{20–22} estimated τ_b (170 ps) as a possible interpretation. Finally, the results presented and discussed in the case of ZnO single crystals produced by chemical vapor transport growth³⁰ are still less conclusive than those presented for the hydrothermally grown ZnO crystals. Although all materials have even been investigated as a function of temperature, it is impossible to follow the given discussion without having a com-

plete chemical analysis showing all detectable impurities and their real concentrations. The general statements that impurity concentrations are less than 10^{17} cm^{-3} , except Li (10^{18} cm^{-3} in hydrothermally grown samples) and H (no concentration mentioned at all), does not allow a complete understanding of the given results.

More recently, a further positron lifetime study of ZnO bulk samples and their annealing under different atmospheres (overpressure of zinc or oxygen, vacuum) has been published.³¹ All these measurements have been performed with an overall time resolution of 270 ps and a statistics of $(1.7\text{--}2.0) \times 10^6$ overall counts. Although these conditions compare well to the ones, from which a ZnO bulk lifetime of (151 ± 2) ps has been derived,¹⁴ the authors consider this difficult to compare in a straightforward way with their directly measured value. Furthermore, no chemical analysis of the ZnO material is given which makes it difficult to identify the true nature of the ionic trapping centers observed at lower temperatures. Finally, results of theoretical calculations of bulk and defect states in ZnO (Ref. 14) are not considered in the discussion.

Other PAS methods, being sensitive to the momentum distribution of the annihilating electrons,^{11–13} have been successfully applied to the study and characterization of various ZnO materials. Examples can be found, e.g., in Refs. 14 and 32–35. In the latter paper,³⁵ the nature of simple native defects in ZnO and their role regarding optical transmission behavior has been demonstrated and discussed using a monoenergetic positron beam. However, any quantitative analysis remains very difficult as it always requires the combination with, e.g., electrical methods. This has been demonstrated, e.g., in Ref. 14, although there had to be made assumptions too about the type of native defects being detected. In general, it has to be stated that due to the lack of a defect-free ZnO reference material in most cases just a comparative analysis regarding the presence and change in concentration of open volume defects is possible.^{32–35}

A more recent article by Zubiaga *et al.*³⁶ deals with an investigation of O^+ -irradiation of ZnO layers deposited on an *a*-sapphire substrate using the Doppler broadening of annihilation radiation of monoenergetic positrons in combination with sheet resistance measurements. The discussion of results is based on an interpretation regarding the plain Zn vacancy given previously²⁰ and presented as its further confirmation. However, this implies that the authors previously possessed a defect-free ZnO crystal which is characterized by a 170 ps bulk lifetime. Although the authors are aware of a different interpretation (of the bulk and defect lifetimes) given in Ref. 14, they do not discuss this further.

Very recently,^{37,38} the formation of open volume defects in ZnO obtained from Scientific Production/Co. Goodwill (Russia) upon electron-irradiation and postirradiation annealing has been reported and discussed. These works concentrate on the identification of secondary defects formed upon annealing using an EP ZnO single crystal as the highest quality standard available. The single positron lifetime observed in the virgin material is given to be 183 ps approximately, with a remark to see no defect components. In our opinion, such a statement implies that this observed lifetime represents the defect-free bulk. Although the identification of sec-

ondary defects is certainly an interesting and important task, the yet unresolved issue of the true bulk lifetime of ZnO will have an influence on the final identification of any secondary defect as well. To summarize, it is found that no clear picture regarding the real τ_b exists, and it appears to be a common practice in the available literature to give reference just to those previous publications which are supportive of an assumed view.

In this respect, it is worth mentioning the work of Tanaka *et al.*³⁹ where the “bulk” lifetime of MgO materials was shown to depend strongly on Ga doping. When the Ga content is negligible, the bulk lifetime can be extracted from measured data using the simple trapping model. This derived bulk lifetime agrees well with the value predicted from calculations (see also Ref. 40). Consequently, comprehensive state-of-the-art calculations of bulk and defect properties at the same scheme should be generally applied to the explanation of experimental data—and vice versa, existing experimental data have to be used not only to scale but also challenge improvements of such, and similar,^{27,39} calculations. This way, finally calculations and experiment might be directly comparable.

Furthermore, an estimation of the true hydrogen content of the ZnO materials under investigation is absolutely necessary to check and possibly support existing ideas from theory^{41,42} about its possible role in the ZnO lattice. Generally it can be noticed that papers in which hydrogen detection by secondary-ion-mass spectroscopy (SIMS) is described do not touch upon the sensitivity and background level of H during SIMS analysis as they are focusing mostly on H depth profiling. Furthermore, it is common practice to calibrate SIMS measurements either by nuclear reaction analysis (NRA) or by well-defined standards produced by ion implantation of H into a given material.^{43,44} However, this seems to be impractical in the case of ZnO simply because the initial H concentration has been found to be already very large.³⁴ In Ref. 34 results of electrochemical H loading of ZnO are presented and discussed. NRA has been used to estimate the H concentration before and after this loading. In addition, from Faraday’s law the H content after loading could be determined independently and was found in good agreement with NRA results. Therefore, NRA is the method of choice in this work to characterize the various ZnO single crystals in their virgin state.

Let us finally consider how the evolution of our techniques for measurement and data analysis, and consideration of possible differences in earlier results from different laboratories, have informed, and been incorporated into, the present study. First, as metallic contacts are essential for studying electrical properties of a ZnO sample, an investigation has been conducted upon a chemical H_2O_2 pretreatment of a ZnO single crystal before sputtering an Au contact on it.^{45–47} It has been found that this pretreatment results in a defective interfacial region where V_{Zn} -related open volume defects are formed. Due to the mentioned pretreatment, the contact changed from an Ohmic to a rectifying behavior with a lower leakage current. Another work⁴⁸ has repeatedly demonstrated that open volume damage created by N^+ ion implantation into a hydrothermally grown ZnO single crystal is clearly detectable by using a monoenergetic positron beam,

and that its depth distribution and change upon annealing can be determined. However, due to the lack of a defect-free ZnO reference, no further characterization of this damage could be given. In addition, beside an electrical characterization by Hall measurements, the positron lifetime in the virgin material has been estimated to be 182 ps. As this positron lifetime value has already previously been assumed to be connected with a ($V_{\text{Zn}}+1\text{H}$) defect,¹⁵ the very first and still rough theoretical calculation given there has now been improved by relaxing the geometry of ($V_{\text{Zn}}+1\text{H}$). This resulted in a theoretical value of ~ 180 ps for the considered configuration. Finally, positron lifetime measurements⁴⁹ at two hydrothermally grown ZnO single crystals from two different producers gave values of 198 ± 1 ps and 181 ± 1 ps for these crystals, respectively. The lifetimes have been attributed to different V_{Zn} -related defects, without being more specific regarding their possible microstructures. It has to be remarked that the crystal having the longer lifetime has been investigated at the Hong Kong laboratory, whereas the other crystal has been measured at Prague.

The latter paper⁴⁹ pointed out the possibility that measuring conditions in different laboratories might have a larger-than-expected influence on the results obtained. Thus, more rigorous research has been initiated on two types of available ZnO single crystals: hydrothermally grown (HTG) and melt grown (MG). Furthermore, not just state-of-the-art positron lifetime measurements of all crystals and their evaluation at just one laboratory have been performed since then, but also a full chemical analysis of each material in order to determine the detailed content of any impurities and their corresponding concentrations. In addition, each crystal has been characterized by x-ray diffraction measurements regarding its orientation and internal stresses. To account for the possible influence of hydrogen on properties of ZnO—as it is ongoing debated in the literature—an experimental estimation of the real H content of each crystal has been performed also by nuclear reaction analysis. Last but not least, further improvements in *ab initio* calculations have been worked out that allowed not only to improve a calculation of the bulk positron lifetime in ZnO but also of various configurations of open volume structural defects without and with hydrogen. The results of all these efforts and work performed are now collected in this paper.

As there are numerous positron studies devoted to ZnO, we have focused on specific aspects of the problem. In general, we have investigated commercially available bulk ZnO materials in their “as prepared” (virgin) state. We have not yet studied thin films or layers that may exhibit substantially different properties compared to bulk materials. Furthermore, we have focused on the grown-in defects of the bulk materials. Defects created by any kind of irradiation are not the subject of the present study, though we may comment on such studies if there is a relation to the present work.

The paper is organized as follows: in Sec. II experimental details are given, Sec. III describes briefly methods used for structural relaxations and positron calculations for the crystal bulk and selected defects, and in Sec. IV the experimental and theoretical results are presented and discussed. Conclusions are drawn in Sec. V.

II. EXPERIMENTAL

Single crystals typically of dimensions $10 \times 10 \times 0.5$ mm³ have been investigated. Ten HTG samples were supplied in 2006 by MaTecK GmbH (Jülich) (MT-06), with their O-face polished. An HTG pair bought in 2004 (MT-04) has been studied previously.³² Further pairs of HTG crystals were sourced from CrysTec GmbH (Berlin) (CT), University Wafers (South Boston/MA) (UW), and Altramet (Atomergic Chemetals Corp., Farmingdale/NY) (AM). Pairs of MG crystals originated from Cermet Inc. (Atlanta/GA) (CM) in 2006, and IKZ (Berlin) (B12, B13). The former were grown without using a crucible, and the latter by the Bridgman method.⁵⁰

Chemical compositions have been estimated by inductively coupled plasma mass spectrometry (ICP-MS) using a Perkin-Elmer ELAN-9000 spectrometer, with results given in Table I. The H content has been determined by standard NRA (Ref. 51) using 6.64 MeV ¹⁵N ions, as successfully demonstrated earlier for HTG ZnO nanorods.³³ Here, NRA (depth resolution ~ 5 nm, hydrogen detection limit: ~ 200 ppm) is generally performed at a depth of ~ 100 nm, as estimated by SRIM calculations,⁵² which guarantees that volume properties, without any influence of surface contaminations, are being studied.

From SRIM it is also found that the analyzing ¹⁵N ions lose their kinetic energy E with increasing penetration depth x mainly by electronic stopping $[(dE/dx)_{\text{electronic}} = 2.52 \text{ keV nm}^{-1}]$, whereas nuclear stopping is about 3 orders of magnitude smaller $[(dE/dx)_{\text{nuclear}} = 0.006 \text{ keV nm}^{-1}]$. This energy transfer to the crystal during analysis can be sufficient to release a weekly bound hydrogen atom from its bonding site, so that it will be able to start diffusion. It is generally assumed that single H atoms would be trapped again immediately so that this diffusion should most probably take place in the form of H₂ molecules. As this diffusing hydrogen is then no longer available at the point of the analysis, this is seen as a drop in concentration with increasing ¹⁵N fluence. Throughout this paper we will call this “unbound H (H-u).” All H atoms which are not moving during analysis, because the energy transfer is not sufficient to release them from their bonding site, will be called “bound H (H-b)” throughout this paper. However, it has to be clearly stated that from NRA it is impossible to draw any conclusion on the kind of bonding of H atoms in the crystal.

The quality of all the crystals studied has been checked by high-resolution x-ray investigations using a Seifert-GE HRD3003PTS. The Cu radiation was monochromatized using a Ge (220) Bartels-type monochromator, having a point focus with a resulting illuminated area of 1.5 mm². To achieve high resolution in reciprocal space, a triple axis analyzer Ge (220) crystal was used. The accuracy of the experimental setup is better than 0.0005 degree. The orientation of all samples was $\langle 001 \rangle$, and the measurements were carried out at the (004) Bragg reflection, i.e., the c -axis lattice constant was measured.

All positron lifetime measurements were performed at room temperature by a fast-fast spectrometer having a timing resolution of 160 ps (Ref. 53) [full width at half maximum (FWHM) ²²Na], and collecting $\sim 10^7$ events per spectrum.

TABLE I. Chemical compositions (volume concentration, in 10^{17} cm^{-3} units) and H content (in at. %; H-b, H-u, H-a stand for H concentrations in “bound,” “unbound,” and “bound-after-annealing” states, respectively) of HTG and MG ZnO crystals. “0.00” means that the corresponding element was detected, but rounding gives zero concentration within the given precision; underlined numbers specify upper limits.

Sample	Li	Mg	Al	Ti	V	Cr	Mn	Fe	Co	Ni
MT-04	0.33	3.32		<u>0.71</u>	<u>0.07</u>	<u>0.07</u>	0.07	<u>0.61</u>	0.03	6.93
MT-06			80.6				0.27		0.12	1.11
UW	5.37					<u>0.01</u>	0.30		0.04	3.67
AM	6.25					<u>0.01</u>	0.65		0.11	0.40
CT			19.4			0.25				0.80
CM-06						<u>0.01</u>				0.22
B12						<u>0.01</u>			0.03	0.12
B13	0.14					<u>0.01</u>			0.05	0.13
Sample	Cu	Ga	Rb	Sr	Zr	Mo	Ag	Cd	In	Sn
MT-04	3.09	0.06					0.14	2.05	<u>0.03</u>	
MT-06	0.95			0.09				0.03		
UW	0.43	0.54	0.01			0.00	0.43	0.17	0.01	
AM	0.37	0.56	0.01		0.29	0.00	0.16	0.11	0.00	0.11
CT	0.69	1.08	0.02				0.16	1.89		
CM-06	0.34	0.43	0.01			0.00	0.16	0.17	1.54	0.01
B12	0.65	0.60	0.01		0.09	0.00	0.17			0.46
B13	0.51	0.58	0.01			0.00	0.15			
Sample	Sb	Te	Pt	Pb	Bi	H-b	H-u	H-a		
MT-04			0.03	0.07	0.04	0.7	1.9	0.3		
MT-06						0.3		0.3		
UW	0.00			0.01		0.8	1.7			
AM	0.00	0.04		0.01		0.5				
CT				0.04		0.3		0.3		
CM-06	0.00	0.04		0.09		0.5				
B12	0.00	0.04		0.66		0.4				
B13	0.00	0.04		0.01		0.5	0.7			

III. COMPUTATIONAL METHODS

Ideas on how to incorporate hydrogen atoms into the ZnO lattice can be found in Refs. 41, 42, and 54. The hexagonal structure of ZnO is enlightened in Fig. 1 and it is useful to consider this structure as a network of ZnO_4 tetrahedra being interconnected at their corners. Van de Walle⁴¹ examined theoretically interstitial hydrogen in ZnO and found that H atoms can be located in several positions in the lattice. First, these are “bond-center” (BC) positions in which H atoms are located approximately in the middle of the original Zn-O bonds (inside corresponding ZnO_4 tetrahedron; see Fig. 1), which cause a substantial lattice distortion at the place of defects. Second, there also exist “antibonding” positions where the H bond is located outside ZnO_4 tetrahedra. Furthermore, hydrogen atoms may occupy vacancies on both, i.e., Zn and O, sublattices as suggested in Refs. 42 and 54. In addition, weakly bound H atoms (in the form of H_2 molecules) may reside in “channels” (along the hexagonal axis c) in the ZnO structure.⁴¹

Now, selected vacancylike defects and hydrogen-vacancy complexes have been studied theoretically using an *ab initio* pseudopotential method. Realistic configurations of such defects were obtained by means of relaxing the total energy of appropriate supercells with respect to atomic positions. In particular, the Vienna *ab initio* simulation package (VASP)⁵⁵ was employed for this purpose. In the course of calculations, projector augmented-wave potentials within the local-density approximation were used.⁵⁶ 96 atom-based supercells containing defects were utilized.

Starting configurations of studied defects were prepared as follows: vacancies were created by removing the corresponding atoms, whereas H atoms were placed into positions inside vacancies, as suggested in Refs. 41 and 42. In particular, we studied the oxygen vacancy (V_{O}) and V_{O} filled with oxygen (H_{O}) as well as the zinc vacancy with no, one, two, and three hydrogen atoms (V_{Zn} , $V_{\text{Zn}}+1\text{H}$, $V_{\text{Zn}}+2\text{H}$, $V_{\text{Zn}}+3\text{H}$, respectively). The notation used to describe configurations of $V_{\text{Zn}}+n\text{H}$ defects ($n=1,2,3$) in the rest of the paper

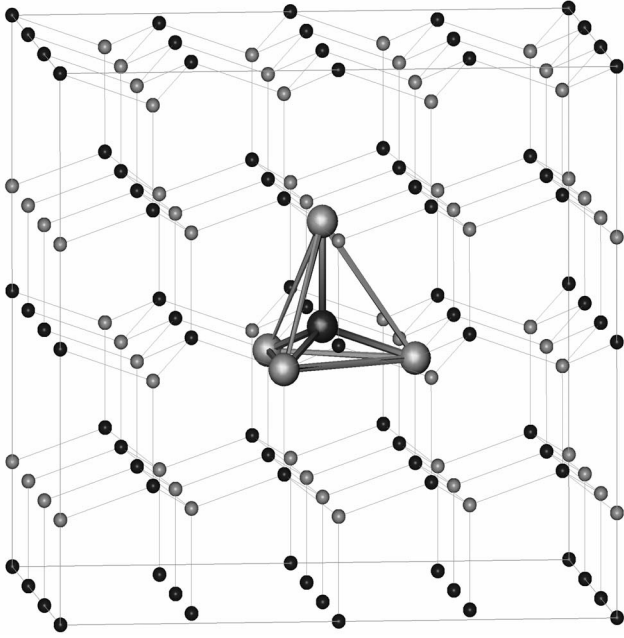


FIG. 1. Perfect ZnO lattice (hexagonal, wurtzite) together with a ZnO_4 tetrahedron. Light (dark) spheres mark O (Zn) atoms.

is as follows: when a H atom is in the position with the O-H bond along the c axis (BC_{\parallel} position after Ref. 41), then “c” is appended to the defect designation. When one or more H atoms form O-H bonds that are not along the c axis (BC_{\perp} positions), then “ab” is appended (the bonds have nonzero projection to the hexagonal basal plane ab). For example, $V_{\text{Zn}}+2\text{H abc}$ marks a defect where one H atom is in the BC_{\parallel} position and the other H atom in the BC_{\perp} one.

At this stage of research we considered the neutral charge state of defects only. As a reference, the perfect ZnO lattice was also considered.

Positron calculations have been performed using a real space method as implemented in the atomic superposition method.⁵⁷ Two approaches were adopted: (i) self-consistent valence charge densities and Coulomb potentials as produced by VASP were considered for valence electrons, whereas the superposition of atomic densities and potentials was considered for core electrons (abbreviated further as SC case), and (ii) superimposed atomic densities and potentials were employed to approximate the electron density and Coulomb potential for both valence and core electrons (NS case). Furthermore, we examined differences between respective nonrelaxed (NR) and relaxed (RE) defect configurations, the former being starting defect configurations described above. In order to study the effect of various approximations, for each defect we performed a set of positron calculations described as follows: NS NR, NS RE, and SC RE.

Finally, positron-induced forces acting on atoms around the defect were implemented according to the scheme developed by Makkonen *et al.*⁵⁸ In such calculations, the so-called conventional scheme^{58,59} for positron calculations is considered, which means that the electronic structure is not primarily influenced by the presence of the positron trapped in a defect. On the other hand, the positions of ions (Zn, O, and H) are influenced by the presence of the positron through

positron-induced forces (PF). These forces are calculated using the Hellman-Feynman theorem employing atomic densities and Coulomb potentials, but the positron density is calculated within the SC scheme described above (this calculation is further marked by SC RE PF). In positron calculations, the approach of Boroński-Nieminen⁶⁰ to the electron-positron correlations and enhancement factor—with the correction⁶¹ for incomplete positron screening with the high frequency dielectric constant $\epsilon_{\infty}=4$ —has been used (referred further to as the BN approach).

As many defects in ZnO are not deep positron traps and supercells used in VASP calculations are rather small, VASP supercells were extended by adding atoms at sides of such supercells when calculating the final positron lifetime and positron energy. Such added atoms were arranged in the form of the regular ZnO lattice. Usually, 2592 atom supercells have been used. In addition, the procedure according to Korhonen *et al.*⁶² was employed to minimize the effect of the finite supercell size on calculated positron properties. The positron binding energy to a defect was obtained as a difference of the ground-state positron energies for the bulk and corresponding defect.

We further refer to Refs. 58 and 59 concerning the theoretical background of positron calculations and to Ref. 14 regarding our previous calculations for ZnO. All computational details of our current method will be given elsewhere.

IV. RESULTS AND DISCUSSION

A. Check of crystal quality

In Fig. 2, reciprocal space maps measured at the (004) Bragg reflection are shown. An almost perfect single crystal has been found in the CT sample. The diffuse scattering around the Bragg peak is very weak; the crystal truncation rod (2Θ - Θ -line at $\Delta\Omega=0$) can be clearly identified. For comparison we also show a (004) reflection of a Si sample in Fig. 2(h). All other ZnO crystals show either a mosaic structure, i.e., a microtexture (MT-06, AM, CM), or even disintegrated into several macroscopic large crystals (UW, B12, B13) and being disoriented one from the other and separated by dislocation walls at the grain boundaries. Partially, these grains are perfect as the CT sample is indicating a size of these “perfect grains” of several microns. On the other hand, in some samples or grains (MT-06, UW, AM) a homogeneous lattice expansion was found. The lattice expansion itself was measured at different Bragg reflections corresponding to different orientations.

Figure 3(a) shows an x-ray pattern of the asymmetrical (114) reflection of sample B12. Again, two macroscopic grains separated by 0.1° can be clearly identified that are embedded into the mosaic structure picture. This intensity distribution does not follow the line of an ideal mosaic crystal (dotted line) and may be caused by the strained regions of the crystal.

Figure 3(b) shows Θ - 2Θ scans that demonstrate again the differences in the investigated samples. The lattice expansion may be caused by an excess of interstitial (impurity) atoms. For specimen MT-06, a strained region with a lattice expansion

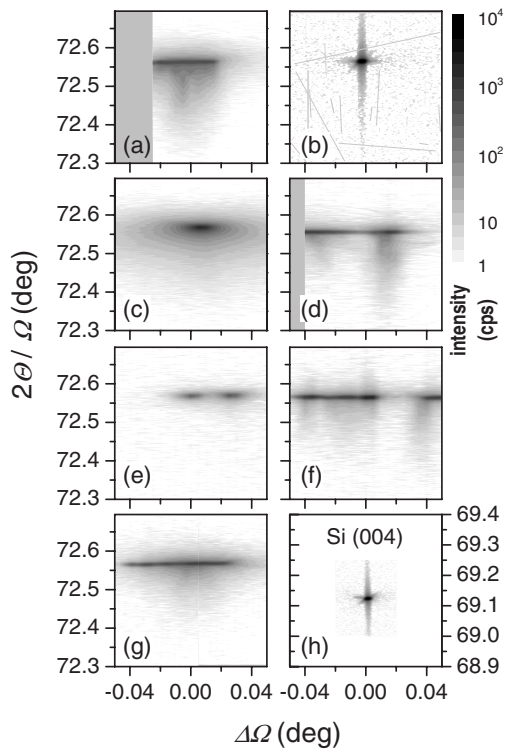


FIG. 2. Reciprocal space maps measured at the (004) Bragg reflection of different ZnO crystals. The correspondence of subfigures to samples is as follows: (a)—MT-06, (b)—CT, (c)—AM, (d)—UW, (e)—B13, (f)—B12, (g)—CM, and (h)—Si(001).

sion of up to 1%, decaying exponentially over of a size of several 100 nm, was found.

The inset of Fig. 3(b) does show the c -lattice constant variation together with the FWHM of the Θ - 2Θ scans, for which a nominal value of 5.20661 Å (Ref. 64) was assumed. Taking into account a FWHM of the Darwin curve of an ideal crystal (0.0035 deg), the crystallite size perpendicular to the sample surface should be around 10 μm , except for MT-06 and AM where we found about 5 μm . In both figures (a+b). A Si (004) reflection is shown for comparison. Measured c -lattice constants vary slightly within a range of 0.0001 nm. Taking a temperature stability of 1 K and a thermal expansion coefficient of $\sim 10^{-5} \text{ K}^{-1}$, this variation seems to be sample specific and may therefore be attributed to the growth process itself (the error bar is almost smaller than 20% of the measured lattice constant variation).

B. Estimation of H content

In Fig. 4, as an example the obtained H concentration for an MT-04 sample is presented. The observed decrease with increasing bombardment by ^{15}N ions finally reaches a constant level of ~ 0.7 at. % ($\sim 5.8 \times 10^{20} \text{ cm}^{-3}$), implying that this amount of H-b in the sample. An extrapolation to the yield at the beginning of the ^{15}N bombardment gives the total H concentration of ~ 2.6 at. % ($\sim 2.2 \times 10^{21} \text{ cm}^{-3}$), and by subtraction of H-b the concentration of H-u, i.e., ~ 1.9 at. % ($\sim 1.6 \times 10^{21} \text{ cm}^{-3}$), is found. In Table I, the measured amounts of H in all samples are given. Values are

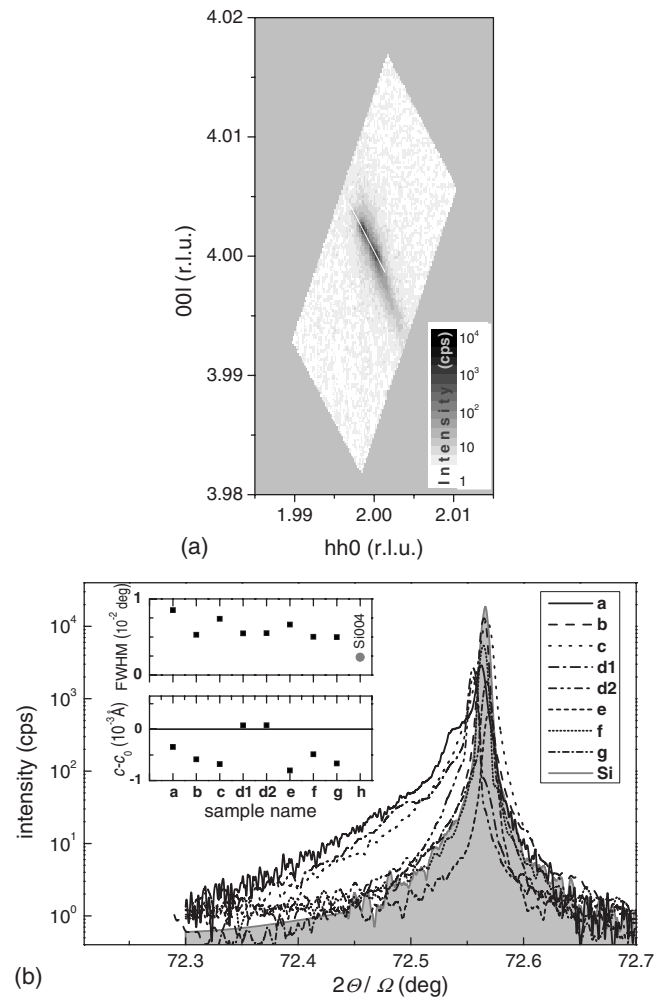


FIG. 3. (a) X-ray pattern of the asymmetrical (114) reflection of sample B12. (At the axes, the chosen unit is 'r.l.u.' = reciprocal lattice units, for which nominal values of $a=3.24982$ Å and $c=5.20661$ Å (Ref. 64) were assumed.) (b) Θ - 2Θ scans of different ZnO crystals. Inserted figures show the c -lattice constant variation with respect to a reference value from the literature (Ref. 63) together with the FWHM of the Θ - 2Θ scans, for which a nominal value of 5.20661 Å (Ref. 64) was assumed. The sample designations a, b, c, d, e, f, g, and h are the same as in Fig. 2. In the case of the UW sample, two crystals visible in Fig. 2(d) (labeled d1 and d2) were investigated.

remarkably large in both types of crystals, and thus need to be seriously considered in any future studies.

Annealing (500 °C, 1 h, air) should remove H-u completely from the ZnO lattice.⁶⁵ Indeed, just 0.3 at. % of H-b was found in MT-04 immediately after such annealing. The slight drop in this value, compared to the as-grown state, indicates involvement of several bonding states, some of them being bound more tightly. In Table I, corresponding results for two other samples investigated (MT-06, CT) are given.

The H concentration for an annealed MT-04 sample versus time is presented in Fig. 5. After a period of 93 d, no change compared to day 1 is observed. However, it shows that after 241 d the H concentration (i.e., ~ 1.9 at. % H-u, and ~ 0.7 at. % H-b) is found to be almost the same as ini-

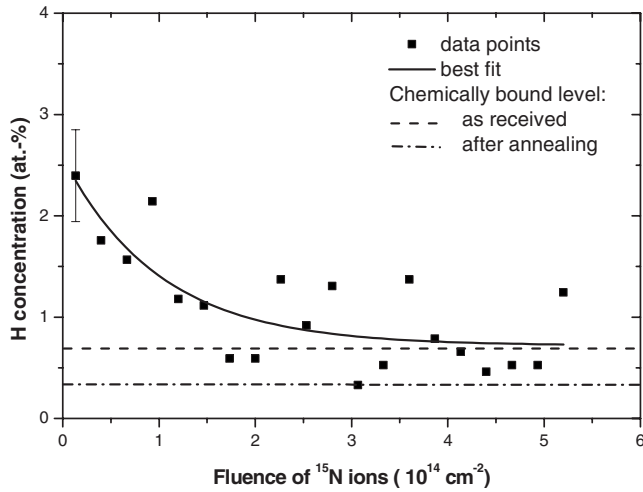


FIG. 4. Hydrogen concentration as a function of the sum of ^{15}N ions used for bombardment during NRA analysis of a MT-04 sample.

tially observed in the as-bought sample. In our opinion, this is a remarkable result. It has to be mentioned that the studied specimen has been kept at all times in an ordinary little specimen box at the office desk, i.e., without any special

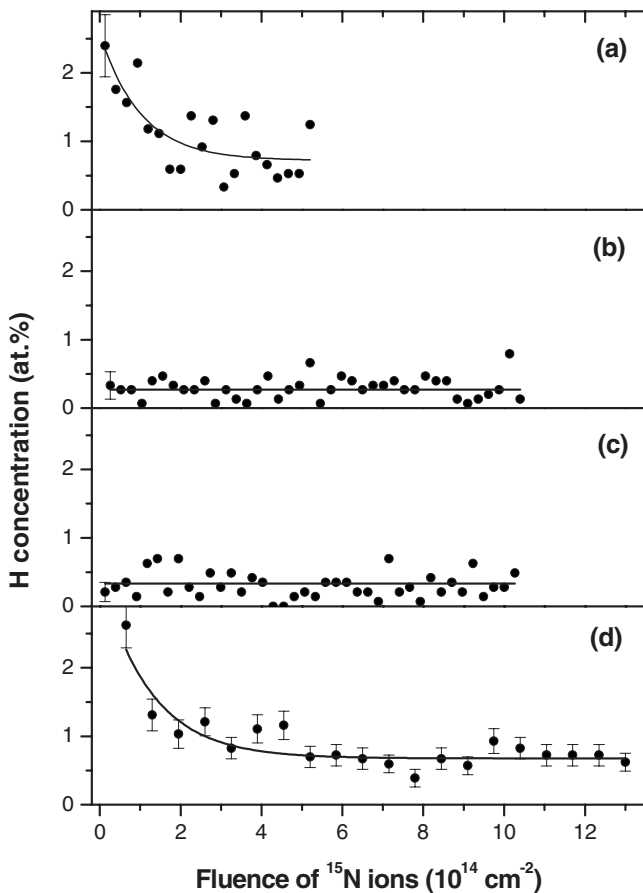


FIG. 5. Hydrogen concentration of a MT-04 sample displayed as a function of time after annealing (500 °C/30 min/air). In (a) the as-received state is shown, whereas (b), (c), and (d) were measured 1, 93, and 241 days after annealing, respectively.

control of humidity. As at FZ Dresden-Rossendorf no air-conditioning of the office rooms is performed, humidity exposed to the sample may have varied with time. During the room heating period covering the first two measuring dates, humidity is expected to be rather stable and of the order $\sim 42\%$. After this period, it may exceed this value depending more or less on outside weather conditions acting through aerating a room by opening of the door or a window, which have not been monitored.

The observed phenomenon of an unintended H uptake by an HTG ZnO single crystal remains to be investigated in detail by well-defined boundary conditions. It might be that the origin of the instability in *p*-type conductivity of ZnO nanorods observed after some time⁹ is connected with such a phenomenon too. On the other hand, it has been demonstrated that a very high total amount of H (up to ~ 30 at. %) can be intentionally introduced into HTG ZnO single crystals by electrochemical doping, where more than half of this amount is found to be H-b, i.e., tightly incorporated into the ZnO crystal lattice.³⁴

C. Positron lifetime measurements

All the as-grown HTG crystals gave a single positron lifetime (in ps) as follows: MT-06 (five pairs, all ± 0.3 ps): 182.0, 181.6, 181.2, 181.7, 181.9; MT-04: 182.1 ± 0.4 (Ref. 32); CT: 181.2 ± 0.2 ; UW: 180.1 ± 0.7 ; AM: 180.5 ± 0.3 ; MT-06 (annealed): 179.7 ± 0.4 . These values are well above $\tau_b = 151 \pm 2$ ps (Ref. 14). The observed drop in lifetime of MT-06 after annealing is negligibly small and possibly due to stress release during heating. Therefore, this annealing does not have any substantial influence on the structure of the defect that causes saturation positron trapping in the HTG crystals. Furthermore, it is concluded that H-u is not related to this yet unknown defect configuration because it is not detected in all crystals investigated (Table I).

MG crystals (as-grown) gave a single positron lifetime also but much shorter than at the HTG crystals (all in ps): CM (bought 2006): 166.4 ± 0.4 ; B12: 165.9 ± 0.2 ; B13: 166.1 ± 0.3 . Again, these values are still above $\tau_b = 151 \pm 2$ ps (Ref. 14).

It is remarkable to see positron lifetimes clustering at 180–182 ps and 165–167 ps for HTG and MG crystals, respectively. This suggests itself that positrons in all the different HTG and MG crystals are trapped in two different but yet unknown open volume defect existing at a concentration sufficiently large to cause saturation trapping. The variety and diversity of impurities in all crystals investigated (Table I) suggests that H-b is most probably connected to these defects.

To be more specific, saturation trapping is known to occur usually for vacancylike defect concentrations larger than 0.01 at. %.¹² All nonhydrogen impurities detected have their concentrations apparently below this limit (Table I) and may hardly influence positron lifetime data even if such impurities would form a complex together with the vacancy. The only exception could be Al impurities found at relatively high concentrations, but in just two types of HTG samples. As the measured positron lifetime for these samples does not

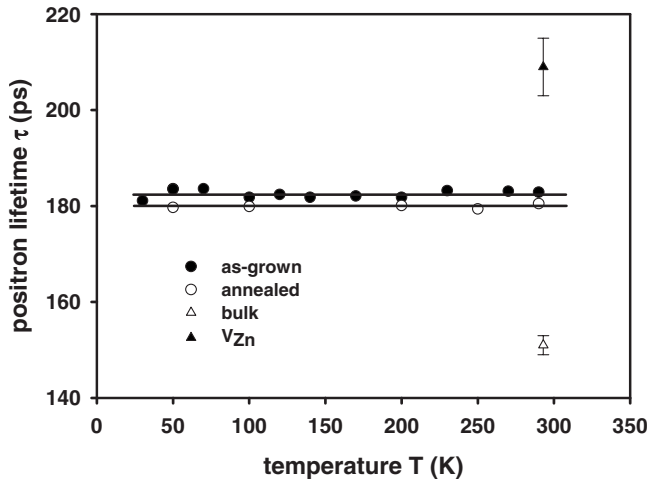


FIG. 6. Positron lifetime of a MT-06 sample displayed as a function of temperature for as-grown state, and after annealing (500 °C/30 min/air).

exhibit any significant deviations from the other lifetimes for HTG samples, we may assume that positrons annihilate in the same type of defects in all HTG samples. NRA results further lead to the conclusion that H-u has no influence upon the positron lifetimes observed (Table I).

No temperature dependence of positron lifetime has been observed for an MT-06 pair in as-grown and annealed states (Fig. 6). This does not allow any conjecture about the charge state of the detected defect, because (i) there is still a saturation trapping observed even at the lowest temperature investigated, (ii) a neutral charge state would not change this picture unless the microstructure of the defect itself changes at lower temperatures, and (iii) in case of a negatively charged defect the trapping efficiency would simply increase with lowering of the temperature due to the $T^{-1/2}$ dependency of the corresponding trapping cross section. If (iii) is relevant, this would have no effect on the measured lifetime because saturation trapping is observed already at RT.

D. Investigation of a former MG ZnO specimen

It has been noticed that a pair of MG crystals bought from Cermet Inc. (Atlanta/GA) (CM-06) in 2006 exhibits just a single positron lifetime of 166.4 ± 0.4 ps, whereas a pair of crystals obtained from the same company in 2002 (CM-02) exhibited a two component spectrum with the following positron lifetimes and intensities: $\tau_1 = (93 \pm 3)$ ps, $\tau_2 = (257 \pm 2)$ ps, $I_1 = (39.9 \pm 0.7)\%$, and $I_2 = (60.1 \pm 0.7)\%$ (Ref. 14). This effect might be connected with reported improvements in crystal growth.²⁵

Nevertheless, it seemed to be of high interest to see if there would be found substantial differences in the crystal purity and H content between samples CM-02 and CM-06 which might explain the observed differences in positron lifetime data. Fortunately, there were remaining pieces of CM-02 kept from the past investigations, and thus the chemical composition could still be estimated. The result and its comparison with a CM-06 sample are given in Table II. It is obvious that both samples differ in their chemical composition. However, as already found in case of other single crystals collected in Table I, the amount of H-b (~ 0.5 at. %) in the volume of a remain from the CM-02 sample is dominating compared to the variety and diversity of all other impurities (Table II), and thus it is impossible to assign a special impurity to be responsible for the differences observed in the positron lifetime spectra. It has to be mentioned also that remains from a CM-02 sample were covered with unremovable metallic contacts, i.e., a sputtered Au layer on the back side and sputtered Pd dots on the front side.⁶⁶ Thus, no specification may be given in Table II regarding possible Au and Pd impurities in the previous CM-02 sample.

NRA performed at remain from a CM-02 sample has been conducted at its back side before it was used in the destructive ICP-MS chemical analysis. The bombardment by ^{15}N ions has been done with increasing kinetic energy in order to perform a depth analysis, i.e., the ions first see the Au layer before finally reaching the ZnO substrate. As the thickness of the sputtered Au layer was known by a rough guess only to be of the order 80–100 nm, its exact value has been estimated to equal 145 nm by standard Rutherford backscattering analysis⁶⁷ using a value of $\rho = 19.3$ g cm⁻³ for the density of crystalline Au. Results of NRA at the CM-02 are presented in Fig. 7.

The estimated H-b depth profile shows some very interesting features. First, the sputtered Au layer has been found to contain a substantial amount of H. This result has been unexpected at first sight because it was reported⁶⁸ that the H solubility in crystalline Au ranges from 4.5×10^{-4} at. % at 1000 °C down to 1.55×10^{-4} at. % at 700 °C at 1 bar pressure, i.e., at room temperature it is almost zero. However, recent more detailed research (see Ref. 69 for a review) has revealed that H may be trapped at all types of open volume defects. In particular, a substantially enhanced H solubility was found in nanocrystalline metals containing a significant volume fraction of grain interfaces which can accumulate more H than a regular lattice, e.g., Pd.⁷⁰ Recent defect studies of thin films^{71,72} revealed that sputtering at room temperature produces such nanocrystalline structure with a high density of open-volume defects. It was also demonstrated that the H solubility in nanocrystalline films is substantially enhanced.⁷¹ Thus, an average H content of ~ 1.8 at. % as

TABLE II. Comparison of chemical compositions (volume concentration, in 10^{17} cm⁻³ units) estimated for CM-02 and CM-06 samples. No specification may be given regarding Au and Pd impurities for the CM-02 sample—see text for explanation.

Sample	Cr	Ni	Cu	Ga	Rb	Mo	Ag	Cd	In	Sn	Sb	Te	Pb
CM-02		1.19	13.66	0.80				0.21					0.13
CM-06	0.01	0.22	0.34	0.43	0.01	0.00	0.16	0.17	1.54	0.01	0.00	0.04	0.09

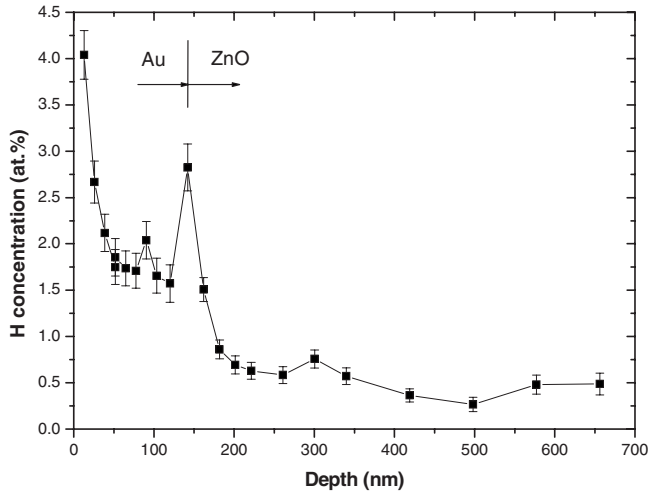


FIG. 7. Hydrogen concentration of a CM-02 sample having a sputtered Au contact displayed as a function of depth.

observed in the sputtered Au layer looks normal and points to the existence of open volume defects in the layer. Toward the surface and the interface of the Au layer, this amount is found to be still much higher. The origin of the H content may be guessed at this moment only—perhaps an uptake from the air, as described above in case of the MT-04 sample, took place. However, the real process remains to be investigated but this finding is helpful to better understand the behavior of metallic contacts on ZnO—see, e.g., Refs. 45–47.

Second, when commenting the H content of the CM-02 sample it has to be reminded that from slow positron implantation spectroscopy has been estimated¹⁴ that a damaged subsurface layer introduced by lapping at the back side (zinc face) exists which does extend as deep as $d = (1942 \pm 32)$ nm. It is reasonable to assume that the rise of the H concentration near the interface with the sputtered Au contact is due to some additional damage caused by the sputtered ions. Indeed, away from this interface behavior a still enhanced H concentration can be noticed in the sample roughly up to a depth of about 300 nm. At larger depth, certainly some bulk level is reached which amounts to $\sim(0.3\text{--}0.5)$ at. %. The remain from a CM-02 sample has

been annealed previously,¹⁴ but over the long time since then an uptake of H might have happened, as observed for sample MT-04 as described above. Thus, the bulk level of H concentration looks comparable to the numbers found in various other ZnO crystals of completely different origin (Table I).

To summarize, the final reason for the clearly observed difference in the positron lifetime spectra of CM-02 (Ref. 14) and CM-06 remains undisclosed.

E. Calculation of bulk and defect positron states

As for the delocalized positron state, recent positron calculations¹⁴ yielded a ZnO bulk lifetime of 159 ps, which is now replaced by a value of 154 ps (see Table III)—obtained with the refined method described above—that is somewhat closer to the experimental value (151 ± 2) ps (Ref. 14) (see also Refs. 18 and 40). Theoretical calculations using the BN approach thus give a lifetime value that is very close to that observed in experiment, and using this approach in defect calculations is therefore justified. In Ref. 27 the bulk lifetime is calculated to be only 144 ps. However, in this case no correction for incomplete positron screening (due to the band gap in ZnO) was used—and our calculations give the same value when the correction described in Ref. 61 is not considered (cf. Ref. 40), which indicates that such a correction is essential to reproduce measured lifetimes.

In this respect we also comment on calculations based on the gradient correction (GC) scheme,⁷³ which was reported in Refs. 14 and 20. The bulk positron lifetime calculated using the GC scheme is 176–177 ps in both works, which does not match well the experimental value given above. For this reason we do not consider the GC scheme in further calculations here. We also note that in the original work of Barbiellini *et al.*⁷³ no oxides were tested though our recent study shows⁷⁴ that in the case of BeO and MgO both BN and GC schemes give comparable results and agree reasonably well with experimental data for delocalized positrons. But further investigations are needed in order to generally justify the GC approach for positron calculations in oxides.

As for the positron distribution in the perfect ZnO lattice, positrons are most probably found in the interstitial channels along the *c* axis of the hexagonal lattice, as deduced from checking the positron density behavior. Hydrogen atoms (in

TABLE III. Results of positron calculations for selected defects; τ and E_b are, respectively, the positron lifetime and binding energy and are given in ps and eV units.

Case	NS NR		NS RE		SC RE		SC RE PF	
	τ	E_b	τ	E_b	τ	E_b	τ	E_b
Bulk			159		154			
V_O	159	~ 0	159	~ 0	154	~ 0	154	~ 0
$V_O + 1H (H_O)$	159	~ 0	159	~ 0	154	~ 0		
V_{Zn}	197	0.34	231	0.60	246	1.25	207	1.11
$V_{Zn} + 1H c$	179	0.12	190	0.19	199	0.48	177	0.25
$V_{Zn} + 1H ab$	178	0.12	194	0.23	203	0.51	179	0.30
$V_{Zn} + 2H abc$	161	~ 0	163	0.01	164	0.03	156	~ 0
$V_{Zn} + 2H ab$	161	~ 0	166	0.02	164	0.03	156	~ 0

the form of H_2 molecules, and perhaps other forms too) can be also present in such regions. Hence, it is instructive to examine to what extent the bulk lifetime could be affected by the presence of hydrogen located in the channels mentioned above.

A brief simulation has been performed in order to check this effect. The ATSUP method was used without taking into account lattice relaxations. It is found that ~ 2 at. % H would cause a shortening of less than 0.5 ps, whereas ~ 25 at. % would result in just ~ 10 ps shortening. Thus it is reasonable to accept that the bulk lifetime (151 ± 2) ps (Ref. 14) (sample CM-02) is not significantly influenced by the (not estimated) presence of H-u, and thus really represents the bulk value. Concerning other interstitial hydrogen positions as predicted in Ref. 41, also just a small H influence on the positron lifetime is expected.

Attempts to assign the experimental positron lifetimes observed in ZnO to specific defects have to take into account the dominant concentration of H, as this is certain now from the NRA results presented. Table III summarizes results of positron lifetime and positron binding energy calculations for bare as well as H-decorated vacancylike defects (first results were presented in Ref. 75). Here, we present results for NS NR, NS RE, SC RE, and SC RE PF computational schemes in order to demonstrate the influence of the effect of various approximations used in computations.

As already shown in Ref. 14 (see also Ref. 27), V_O is too “shallow” to confine a positron. Even if now positron-induced forces are taken into account, the situation does not change. As for an H atom occupying an O site (H_O) (Ref. 42), our calculations revealed—not surprisingly—that it cannot trap positrons, and therefore cannot correspond to any of the observed positron lifetimes even if calculations using positron-induced forces were not carried out here. Thus, we can conclude that both defects, V_O and H_O , are invisible to positrons.

We now discuss in detail results for V_{Zn} that is a substantially deeper positron well for positrons compared to V_O . In Table III, it is demonstrated how various approximations employed in calculations affect the positron behavior. Within the NS scheme, relaxations affect strongly the lifetime (see also Ref. 14) due to a large outward shift of O atoms surrounding the vacancy. When the charge transfer among atoms is taken into account (SC RE scheme), the lifetime is even longer as positrons are attracted to oxygen anions next to the vacancy (though oxygen anions attract positrons, the corresponding electron density is rather low, which results in the increase in the lifetime compared to the NS RE case). Taking into account positron forces results in an inward shift of these anions (as well as of neighboring cations), which reduces the lifetime to 207 ps. This value can be well compared with defect lifetimes (202–209 ps) observed in some electron-irradiated ZnO samples.^{18,40} The calculated positron binding energy slightly exceeds 1 eV (SC RE PF scheme), which confirms quite a deep positron potential well in the place of V_{Zn} in ZnO.

In Ref. 36, a coincidence Doppler broadening profile measured for an O^+ -irradiated ZnO layer is compared with the profile calculated for V_{Zn} (without specifying computational details, which makes it difficult to judge the precision of

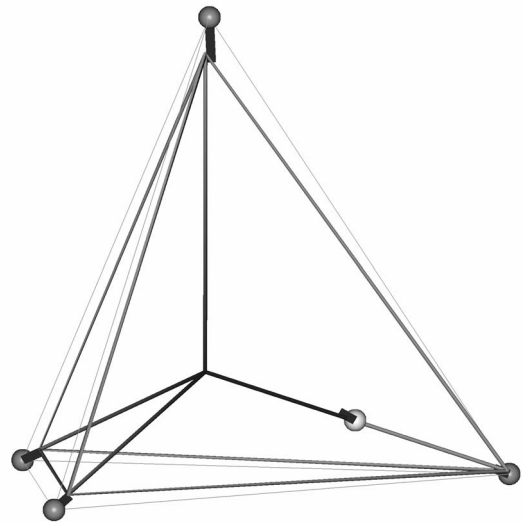


FIG. 8. Atomic configuration of the $V_{Zn}+1H$ ab defect. H atom/sphere has the lightest color; otherwise sphere/atom colors are the same as in Fig. 1. The original (nonrelaxed) ZnO_4 tetrahedron is plotted by solid lines (as in Fig. 1). Spheres and another tetrahedron (thin lines) indicate relaxed positions. Thicker dark bars show atomic shifts due to positron induced forces.

calculations). Both profiles are mentioned to be related to a defect-free bulk. The calculated and experimental ratio curves are claimed to match well, which should indicate that the main defect created in ZnO layers is V_{Zn} . However, no information is given concerning the ZnO reference sample, i.e., a “defect-free” one. In the context of the present work, where we show that defect-free ZnO materials are not currently available, it is obvious that such a defect identification is not well justified.

Next, we study atomic configurations of V_{Zn} containing one H atom, i.e., the $V_{Zn}+1H$ defect. There exist two configurations which differ by the position of the hydrogen atom. Namely, these are $V_{Zn}+1H$ c and $V_{Zn}+1H$ ab configurations. We also tried several different starting configurations with the H atom located inside the $V_{Zn}O_4$ tetrahedron (in addition to those described in Sec. III) and it turned out that regardless of starting positions of the H atom, its final position can be identified with one of the positions described above. In such positions the H atom is close (~ 1 Å) to the nearest O atom, like for the interstitial H.⁴¹ The resulting positron lifetimes (SC RE PF calculation; see Table III) are 177 and 179 ps for $V_{Zn}+1H$ c and $V_{Zn}+1H$ ab configurations, respectively. These values are about 30 ps shorter than for the “bare” V_{Zn} vacancy, which demonstrates the effect of lowering the vacancy free volume due to the incorporation of hydrogen. Correspondingly, the positron binding energies that amount to 0.25 and 0.30 eV for the above two configurations are significantly lower than for V_{Zn} . The effect of the studied computational approximations can be described in the way similar to V_{Zn} , which is also demonstrated in Fig. 8. On the basis of calculated lifetimes, it is suggested that the $V_{Zn}+1H$ defect is responsible for the 180–182 ps lifetime detected in our HTG samples (see Sec. IV C) as well as in HTG samples studied in other works.^{17,37,38}

When two H atoms are present inside V_{Zn} , they occupy two bond-center positions with a slight distortion of the $V_{\text{Zn}}\text{O}_4$ tetrahedron. Again, two nonequivalent configurations for the $V_{\text{Zn}}+2\text{H}$ defect can be found (ab and abc). The results of positron lifetime and binding energy calculations for these configurations are shown in Table III. One can see that for NS NR and SC RE PF calculations $V_{\text{Zn}}+2\text{H}$ defects do not constitute a positron trap, but surprisingly this is not true for the NS RE and SC RE computational schemes. As SC RE PF are considered to be the most precise and elaborated way of calculations, we conclude that any of two possible configurations of the $V_{\text{Zn}}+2\text{H}$ defect most probably does not trap positrons. Thus, already two H atoms are enough to fill up the free volume of V_{Zn} so that it becomes invisible to positrons.

For the sake of completeness, we also performed calculations for $V_{\text{Zn}}+3\text{H}$ defects (there are again two nonequivalent configurations ab and abc). In this case even for NS RE and SC RE computations there is no positron trapping, and we again conclude that $V_{\text{Zn}}+3\text{H}$ defects do not represent positron traps.

So far a reasonable interpretation for the 180–182 ps lifetime observed in HTG samples could be suggested. Concerning the MG samples, where lifetimes in the range 165–167 ps have been found, none of studied defects gives a lifetime that would correspond to those determined in experiment and further studies and considerations are necessary to address this point.

In the present work yet other defect configurations involving H atoms have been studied. It is worth mentioning that the H_2 molecule does not appear to be stable inside V_{Zn} . Similarly, V_{Zn} configurations that involve any of antibonding H sites⁴¹ are either found to be not stable or result in much higher energies than those involving BC sites. For these reasons, it is supposed that such defects almost certainly do not exist in reality and therefore no positron calculations have been performed for them.

However, there can be yet other H-vacancy complexes that could explain the measured lifetimes. In this respect, the role of H in a $V_{\text{Zn}+\text{O}}$ divacancy needs to be investigated. The H_O defect (i.e., $V_\text{O}+1\text{H}$)—as part of a larger complex $\text{H}_\text{O}+V_{\text{Zn}}+n\text{H}$ (with $n=0,1,2,\dots$)—could play a role as well. Further calculations will be required to assess this idea, supposing also the possibility of various charge states of defects which have not been considered in the present work.

F. Relation to other experimental data

So-called “plasma hydrogenation” in ^1H or ^2D atmospheres has gained attention in connection with PL and other investigations—see, e.g., Refs. 76–79. Although conditions of plasma treatment have been carefully reported, no quantitative analysis of the ^1H or ^2D concentration has been performed. Just in Ref. 76, ^1H concentrations in the samples were at least qualitatively analyzed by depth profiling with secondary-ions-mass spectrometry (SIMS). However, most of the analyses were carried out for ^2D plasma-irradiated samples. For the qualitative analyses, the sensitivity of the equipment was calibrated with a standard sample prepared

by ion implantation. For a given sample, the ^2D concentration was found to be nearly constant of the order 10^{17} cm^{-3} in a narrow subsurface range of about 0–30 nm, and to steeply decrease with increasing depth. It is reported also that ^1H does interact in some way with impurities and/or defects in ZnO substrates, and that its diffusion behavior is not simply due to its concentration gradient. However, the question if some subsurface damage of the treated ZnO sample might originate from the plasma treatment itself or not has neither been considered nor discussed.

Other authors⁷⁷ report a complete restoration of the original properties of the sample upon annealing at 450 °C, which from our point of view indicates that ^1H introduced by the plasma treatment could be considered as H-u according to our NRA notification mentioned above. In our opinion, the results obtained by SIMS (Ref. 76) may not be compared directly with the absolute estimations from NRA as reported in Table I though the reason for the discrepancy between the results of NRA and SIMS methods needs to be cleared.

Hydrogen-related defects have also been studied via accessing local vibrational modes (LVM's) of hydrogen atoms (see, e.g., Refs. 80–82). LVM's are dependent on mass, bonding and local environment of impurities, and have been investigated after a plasma treatment of ZnO crystal in either hydrogen or deuterium atmosphere. The $V_{\text{Zn}}+2\text{H}$ defect has seriously been considered to exist by several authors^{80–82} in order to explain results of such experiments. However, as explained above, we do not expect that positrons would be sensitive to this defect and cannot confirm the existence of such defects independently.

As for the $V_{\text{Zn}}+1\text{H}$ complex, to our knowledge it has not been considered yet in LVM studies. However, there is some indication from previous experiments⁷⁹ that such defects could exist; namely, the H-I defect corresponding to the 3611.3 cm^{-1} line remains unaffected with uniaxial stress along the c axis. One of the explanations could be that the O-H bond (along the c axis) inside V_{Zn} is much less affected by stress (as there is a free volume around the H atom compared to the O-H bond for the BC_\parallel hydrogen interstitial position). To check and prove this hypothesis would require theoretical calculations of the corresponding LVM frequency and its dependence on stress.

Due to the well-known effect of preferential positron trapping at defects having the largest open volume among coexisting defects of different size and structure, all the defects proposed in the LVM literature^{80–82} so far may really exist but cannot explain the observed lifetime of ~ 180 ps found for HTG samples. Namely, H-impurity atom complexes (e.g., Li-H, Cu-H, and Na-H^{80–82}), if really formed, can be excluded because: (i) Li is not an impurity found in all our crystals, and furthermore the $V_{\text{Zn}}+\text{Li}$ complex does not represent a positron trap, as proved in the present work by employing the same computational procedure as for H-related complexes, (ii) although Cu impurities are present in all crystals, the $V_{\text{Zn}}+\text{Cu}$ complex probably does not trap positrons as well, due to the noninterstitial character of this impurity, and (iii) for the same reasons the $V_{\text{Zn}}+\text{Na}$ complex can be excluded considering also that Na is not found in all our samples.

V. CONCLUSIONS

An extended investigation of HTG and MG ZnO single crystals, available from different suppliers, has been performed. This regards first a check of the crystal quality by XRD together with a comprehensive estimation of the detailed impurity and hydrogen contents by ICP-MS and NRA, respectively. Second, from all ZnO crystals the positron lifetime spectrum has been measured by using the same high-resolution spectrometer, corresponding very high statistics, and data evaluation procedure in order to avoid any additional uncertainty by using different conditions of investigation.

A variety in the microtexture of all ZnO crystals, with crystallites being generally as large as $5\ \mu\text{m}$ or above, as well as much differing nonhydrogen impurity contents have been observed. Hydrogen in a bound state (H-b) has been detected in all crystals at concentrations exceeding that of nonhydrogen impurities by about 2 orders of magnitude, whereas hydrogen in unbound state (H-u) has not been detected in all ZnO crystals. Positron lifetimes have been found to cluster at 180–182 ps and 165–167 ps for HTG and MG crystals, respectively.

Results from *ab initio* calculations, including the effects of lattice relaxation due to charge transfer as well as positron-induced forces, have been presented for the bulk and various open volume defects connected with hydrogen, like $V_{\text{Zn}}+n\text{H}$ ($n=0,1,2,3$). It has been discussed that saturation trapping at the $V_{\text{Zn}}+1\text{H}$ defect is the most natural explanation for the 180–182 ps positron lifetime observed in HTG crystals, whereas the structure of a defect giving a reasonable explanation of the 165–167 ps positron lifetime found in MG crystals remains to be elucidated from further experiments. The bulk lifetime of 154 ps estimated from the present calculations is now closer to the experimental value of $\tau_b=(151\pm 2)$ ps (Ref. 14). These results are a further sup-

port of the experimental finding and interpretation that the positron bulk lifetime in ZnO should be ~ 150 ps,^{14,18,40} contrary to the repeated conclusion and view from the literature^{19–22,36} that a value of ~ 170 ps should represent the defect-free state.

An attempt to unveil the reason of the different positron lifetime spectrum observed previously¹⁴ and now in a MG crystal of the same supplier has been performed. Thereby, the nonhydrogen impurity content has been determined by ICP-MS, and the distribution of H at an Au/ZnO interface has been determined by NRA as well. Finally, the H content of a HTG crystal upon annealing and time afterward has been monitored. The latter behavior is most probably related to properties of electrical contacts made at ZnO and the instability in *p*-type conductivity observed at ZnO nanorods in literature.

All experimental as well as theoretical findings imply that various types of Zn-vacancy–hydrogen complexes play a role in ZnO and need to be taken into account in future studies. Presented results also demonstrate that the behavior of H in ZnO needs to be further investigated by combining various experimental and theoretical approaches in order to understand its influence on various properties of ZnO, some of them being rather puzzling.

ACKNOWLEDGMENTS

We are grateful to M. J. Puska for his ATSUP code that served as a basis for further developments. The authors thank R. Grötzschel for his RBS measurement to estimate the thickness of an Au layer. This work is part of Research Plan No. MS 0021620834 and Project No. COST OC 165 that are financed by the Ministry of Education of the Czech Republic. This work was financially supported by the Research Grant Council, Hong Kong Special Administrative Region under the schemes of the General Research Fund (Grants No. 7037/06P and No. 7031/08P) and the Germany/Hong Kong Joint Research Scheme (Grant No. G_HK026/07).

¹D. C. Look, *Mater. Sci. Eng.*, B **80**, 383 (2001).

²*Transparent Conducting Oxides*, MRS Bull. Vol. 25, edited by D. S. Ginley and C. Bright (Materials Research Society, Warrendale, PA, 2000), p. 15.

³Ü. Özgür, Ya. I. Alivov, C. Liu, A. Teke, M. A. Reshchikov, S. Dogan, V. Avrutin, S.-J. Cho, and H. Morkoc, *J. Appl. Phys.* **98**, 041301 (2005).

⁴D. C. Look, *J. Electron. Mater.* **35**, 1299 (2006).

⁵H. J. Queisser and E. E. Haller, *Science* **281**, 945 (1998).

⁶G. Bouzerar and T. Ziman, *Phys. Rev. Lett.* **96**, 207602 (2006).

⁷D. Iusan, B. Sanyal, and E. Eriksson, *J. Appl. Phys.* **101**, 09H101 (2007).

⁸R. S. Wang, Q. L. Gu, C. C. Ling, and H. C. Ong, *Appl. Phys. Lett.* **92**, 042105 (2008).

⁹Y. F. Hsu, Y. Y. Xi, K. H. Tam, A. B. Djuricic, J. Luo, C. C. Ling, C. K. Cheung, A. M. C. Ng, W. K. Chan, C. D. Beling, S. Fung, K. W. Cheah, P. W. K. Fong, and C. C. Surya, *Adv. Funct. Mater.* **18**, 1020 (2008).

¹⁰Y. Zhong, A. B. Djuricic, Y. F. Hsu, K. S. Wong, G. Brauer, C. C.

Ling, and W. K. Chan, *J. Phys. Chem. C* **112**, 16286 (2008).

¹¹*Positron Spectroscopy of Solids*, edited by A. Dupasquier and A. P. Mills, Jr. (IOS, Amsterdam, 1995).

¹²R. Krause-Rehberg and H. S. Leipner, *Positron Annihilation in Semiconductors—Defect Studies* (Springer, Berlin, 1999).

¹³*Slow Positron Beam Techniques for Solids and Surfaces*, *Appl. Surf. Sci.*, Vol. 194, edited by G. Brauer and W. Anwand (Elsevier, Amsterdam, 2002).

¹⁴G. Brauer, W. Anwand, W. Skorupa, J. Kuriplach, O. Melikhova, C. Moisson, H. von Wenckstern, H. Schmidt, M. Lorenz, and M. Grundmann, *Phys. Rev. B* **74**, 045208 (2006).

¹⁵G. Brauer, J. Kuriplach, J. Cizek, W. Anwand, O. Melikhova, I. Prochazka, and W. Skorupa, *Vacuum* **81**, 1314 (2007).

¹⁶M. Liu, A. H. Kitai, and P. Mascher, *J. Lumin.* **54**, 35 (1992).

¹⁷S. Brunner, W. Puff, P. Mascher, and A. G. Balogh, in *Microstructural Processes in Irradiated Materials*, edited by S. J. Zinkle, G. E. Lucas, R. C. Ewing, and J. S. Williams, MRS Symposia Proceedings No. 540 (Materials Research Society, Warrendale, PA, 1999), p. 207.

- ¹⁸S. Brunner, W. Puff, A. G. Balogh, and P. Mascher, *Mater. Sci. Forum* **363-365**, 141 (2001).
- ¹⁹F. Tuomisto and D. C. Look, *Proc. SPIE* **6474**, 647413 (2007).
- ²⁰F. Tuomisto, V. Ranki, K. Saarinen, and D. C. Look, *Phys. Rev. Lett.* **91**, 205502 (2003).
- ²¹F. Tuomisto, K. Saarinen, and D. C. Look, *Phys. Status Solidi A* **201**, 2219 (2004).
- ²²F. Tuomisto, K. Saarinen, D. C. Look, and G. C. Farlow, *Phys. Rev. B* **72**, 085206 (2005).
- ²³M. Hakala, M. J. Puska, and R. M. Nieminen, *Phys. Rev. B* **57**, 7621 (1998).
- ²⁴D. C. Look, D. C. Reynolds, J. R. Sizelove, R. L. Jones, C. W. Litton, G. Cantwell, and W. C. Harsch, *Solid State Commun.* **105**, 399 (1998).
- ²⁵D. C. Reynolds, C. W. Litton, D. C. Look, J. E. Hoelscher, B. Clafflin, T. C. Collins, J. Nause, and B. Nemeth, *J. Appl. Phys.* **95**, 4802 (2004).
- ²⁶J. Nause and B. Nemeth, *Semicond. Sci. Technol.* **20**, S45 (2005).
- ²⁷H. Takenaka and D. J. Singh, *Phys. Rev. B* **75**, 241102(R) (2007).
- ²⁸A. Uedono, T. Koida, A. Tsukazaki, M. Kawasaki, Z. Q. Chen, S. F. Chichibu, and H. Koinuma, *J. Appl. Phys.* **93**, 2481 (2003).
- ²⁹K. Ito, T. Oka, Y. Kobayashi, Y. Shirai, K. Wada, M. Matsumoto, M. J. Fujinami, T. Hirade, Y. Honda, H. Hosomi, Y. Nagai, K. Inoue, H. Saito, K. Sakaki, K. Sato, A. Shimazu, and A. Uedono, *J. Appl. Phys.* **104**, 026102 (2008).
- ³⁰F. Tuomisto, K. Saarinen, K. Graszka, and A. Mycielski, *Phys. Status Solidi B* **243**, 794 (2006).
- ³¹A. Zubiaga, F. Plazaola, J. A. Garcia, F. Tuomisto, V. Munoz-Sanjose, and R. Tena-Zaera, *Phys. Rev. B* **76**, 085202 (2007).
- ³²G. Brauer, W. Anwand, W. Skorupa, J. Kuriplach, O. Melikhova, J. Cizek, I. Prochazka, C. Moisson, H. von Wenckstern, H. Schmidt, M. Lorenz, and M. Grundmann, *Superlattices Microstruct.* **42**, 259 (2007).
- ³³G. Brauer, W. Anwand, D. Grambole, W. Skorupa, Y. Hou, A. Andreev, C. Teichert, K. H. Tam, and A. B. Djurisic, *Nanotechnology* **18**, 195301 (2007).
- ³⁴J. Cizek, N. Zaludova, M. Vlach, S. Danis, J. Kuriplach, I. Prochazka, G. Brauer, W. Anwand, D. Grambole, W. Skorupa, R. Gemma, R. Kirchheim, and A. Pundt, *J. Appl. Phys.* **103**, 053508 (2008).
- ³⁵F. A. Selim, M. H. Weber, D. Solodovnikov, and K. G. Lynn, *Phys. Rev. Lett.* **99**, 085502 (2007).
- ³⁶A. Zubiaga, F. Tuomisto, V. A. Coleman, H. H. Tan, C. Jagadish, K. Koike, S. Sasa, M. Inoue, and M. Yano, *Phys. Rev. B* **78**, 035125 (2008).
- ³⁷Z. Q. Chen, K. Betsuyaku, and A. Kawasuso, *Phys. Rev. B* **77**, 113204 (2008).
- ³⁸Z. Q. Chen, S. J. Wang, M. Maekawa, A. Kawasuso, H. Naramoto, X. L. Yuan, and T. Sekiguchi, *Phys. Rev. B* **75**, 245206 (2007).
- ³⁹I. Tanaka, T. Mizoguchi, M. Matsui, S. Yoshiaka, H. Adachi, T. Yamamoto, T. Okajima, M. Umesaki, W. Y. Ching, Y. Inoue, M. Mizuno, H. Araki, and Y. Shirai, *Nature Mater.* **2**, 541 (2003).
- ⁴⁰M. Mizuno, H. Araki, and Y. Shirai, *Mater. Trans.* **45**, 1964 (2004).
- ⁴¹C. G. Van de Walle, *Phys. Rev. Lett.* **85**, 1012 (2000).
- ⁴²A. Janotti and C. G. Van de Walle, *Nature Mater.* **6**, 44 (2007).
- ⁴³A. Eicke and G. Bilger, *Fresenius J. Anal. Chem.* **341**, 214 (1991).
- ⁴⁴F. Pavlyak, *Surf. Interface Anal.* **19**, 232 (2004).
- ⁴⁵X. D. Chen, Q. L. Gu, C. C. Ling, G. Brauer, W. Anwand, W. Skorupa, H. Reuther, and A. B. Djurisic, *Phys. Status Solidi C* **4**, 3633 (2007).
- ⁴⁶Q. L. Gu, C. C. Ling, X. D. Chen, C. K. Cheng, A. M. C. Ng, C. D. Beling, S. Fung, A. B. Djurisic, L. W. Lu, G. Brauer, and H. C. Ong, *Appl. Phys. Lett.* **90**, 122101 (2007).
- ⁴⁷Q. L. Gu, C. K. Cheung, C. C. Ling, A. M. C. Ng, A. B. Djurisic, L. W. Lu, X. D. Chen, S. Fung, C. D. Beling, and H. C. Ong, *J. Appl. Phys.* **103**, 093706 (2008).
- ⁴⁸G. Brauer, W. Anwand, W. Skorupa, J. Kuriplach, O. Melikhova, J. Cizek, I. Prochazka, H. Von Wenckstern, M. Brandt, M. Lorenz, and M. Grundmann, *Phys. Status Solidi C* **4**, 3642 (2007).
- ⁴⁹C. W. Hui, Z. D. Zhang, T. J. Zhou, C. C. Ling, C. D. Beling, S. Fung, G. Brauer, W. Anwand, and W. Skorupa, *Phys. Status Solidi C* **4**, 3672 (2007).
- ⁵⁰D. Schulz, S. Ganschow, D. Klimm, M. Neubert, M. Roßberg, M. Schmidbauer, and R. Fornani, *J. Cryst. Growth* **296**, 27 (2006).
- ⁵¹W. A. Lanford, in *Handbook of Modern Ion Beam Materials Analysis*, edited by R. Tesmer and M. Nastasi (Materials Research Society, Pittsburgh, PA, 1995), p. 193.
- ⁵²J. F. Ziegler, J. P. Biersack, and U. Littmark, *The Stopping and Range of Ions in Solids* (Pergamon, New York, 1985).
- ⁵³F. Becvar, J. Cizek, L. Lestak, I. Novotny, I. Prochazka, and F. Sebesta, *Nucl. Instrum. Methods Phys. Res. A* **443**, 557 (2000).
- ⁵⁴M. G. Wardle, J. P. Goss, and P. R. Briddon, *Phys. Rev. Lett.* **96**, 205504 (2006).
- ⁵⁵G. Kresse and J. Hafner, *Phys. Rev. B* **47**, 558 (1993); **49**, 14251 (1994); G. Kresse and J. Furthmüller, *Comput. Mater. Sci.* **6**, 15 (1996); *Phys. Rev. B* **54**, 11169 (1996).
- ⁵⁶G. Kresse and J. Hafner, *J. Phys.: Condens. Matter* **6**, 8245 (1994); G. Kresse and D. Joubert, *Phys. Rev. B* **59**, 1758 (1999).
- ⁵⁷M. J. Puska, R. M. Nieminen, *J. Phys. F: Met. Phys.* **13**, 333 (1983); A. P. Seitsonen, M. J. Puska, and R. M. Nieminen, *Phys. Rev. B* **51**, 14057 (1995).
- ⁵⁸I. Makkonen, M. Hakala, and M. J. Puska, *Phys. Rev. B* **73**, 035103 (2006).
- ⁵⁹M. J. Puska and R. M. Nieminen, *Rev. Mod. Phys.* **66**, 841 (1994).
- ⁶⁰E. Boronski and R. M. Nieminen, *Phys. Rev. B* **34**, 3820 (1986).
- ⁶¹M. J. Puska, S. Mäkinen, M. Manninen, and R. M. Nieminen, *Phys. Rev. B* **39**, 7666 (1989).
- ⁶²T. Korhonen, M. J. Puska, and R. M. Nieminen, *Phys. Rev. B* **54**, 15016 (1996).
- ⁶³E. H. Kisi and M. M. Elcombe, *Acta Crystallogr. C* **45**, 1867 (1989).
- ⁶⁴H. McMurdie, M. Morris, E. Evans, B. Paretzkin, W. Wong-Ng, L. Ettliger, and C. Hubbard, *Powder Diffr.* **1**, 64 (1986).
- ⁶⁵S. J. Pearton, D. P. Norton, K. Ip, Y. W. Heo, and T. Steiner, *Prog. Mater. Sci.* **50**, 293 (2005).
- ⁶⁶H. von Wenckstern, R. Pickenhain, H. Schmidt, M. Brandt, G. Biehne, M. Lorenz, M. Grundmann, and G. Brauer, *Appl. Phys. Lett.* **89**, 092122 (2006).
- ⁶⁷Hem Raj Verma, *Atomic and Nuclear Analytical Methods* (Springer, Berlin, 2007).
- ⁶⁸C. L. Thomas, *Trans. Soc. Min. Eng. AIME* **239**, 485 (1967).
- ⁶⁹A. Pundt and R. Kirchheim, *Annu. Rev. Mater. Res.* **36**, 555 (2006).

- ⁷⁰T. Mütschele and R. Kirchheim, *Scr. Metall.* **21**, 135 (1987).
- ⁷¹J. Cízek, I. Prochazka, G. Brauer, W. Anwand, A. Mücklich, R. Kirchheim, A. Pundt, C. Bähz, and M. Knapp, *Appl. Surf. Sci.* **252**, 3237 (2006).
- ⁷²J. Cízek, I. Prochazka, S. Danis, O. Melikhova, M. Vlach, N. Zaludova, G. Brauer, W. Anwand, A. Mücklich, R. Gemma, E. Nikitin, R. Kirchheim, and A. Pundt, *J. Alloys Compd.* **446-447**, 484 (2007).
- ⁷³B. Barbiellini, M. J. Puska, T. Torsti, and R. M. Nieminen, *Phys. Rev. B* **51**, 7341 (1995).
- ⁷⁴J. Kuriplach, O. Melikhova, and G. Brauer, *Radiat. Phys. Chem.* **76**, 101 (2007).
- ⁷⁵J. Kuriplach, G. Brauer, O. Melikhova, J. Cizek, I. Prochazka, W. Anwand, and W. Skorupa, *Mater. Sci. Forum* **607**, 117 (2009).
- ⁷⁶N. Ohashi, T. Ishigaki, N. Okada, H. Taguchi, I. Sakaguchi, S. Hishita, T. Sekiguchi, and H. Haneda, *J. Appl. Phys.* **93**, 6386 (2003).
- ⁷⁷Y. M. Strzhemechny, J. Nemergut, P. E. Smith, J. Bae, D. C. Look, and L. J. Brillson, *J. Appl. Phys.* **94**, 4256 (2003).
- ⁷⁸Y. M. Strzhemechny, H. L. Mosbacker, D. C. Look, D. C. Reynolds, C. W. Litton, N. Y. Garces, N. C. Giles, and L. E. Halliburton, *Appl. Phys. Lett.* **84**, 2545 (2004).
- ⁷⁹Y. M. Strzhemechny, H. L. Mosbacker, S. H. Goss, D. C. Look, D. C. Reynolds, C. W. Litton, N. Y. Garces, N. C. Giles, L. E. Halliburton, S. Niki, and L. J. Brillson, *J. Electron. Mater.* **34**, 399 (2005).
- ⁸⁰E. V. Lavrov and J. Weber, *Phys. Rev. B* **73**, 035208 (2006).
- ⁸¹M. G. Wardle, J. P. Goss, and P. R. Briddon, *Appl. Phys. Lett.* **88**, 261906 (2006).
- ⁸²E. V. Lavrov and J. Weber, *Phys. Status Solidi B* **243**, 2657 (2006).